Effect of temperature on corrosion behaviour of N80 steel in CO_2-saturated formation water

Effect of temperature on corrosion behaviour of N80 steel in CO_2-saturated formation water

Z R Ye[1], Z C Qiu[1], R Yi[1], P F Sui[2], X Q Lin[2], K Li[2]

[1] PetroChina Research Institute of Petroleum Exploration & Development, Beijing 100083, PR China
[2] School of Mechanical and Electronic Engineering, China University of Petroleum, Qingdao 266580, PR China

Corresponding author and e-mail: Z R Ye, yezr@petrochina.com.cn

Abstract. Corrosion behaviour of N80 steel in CO_2-saturated formation water was studied by weight loss measurement, electrochemical test and surface characterization. The results showed that the general corrosion rate initially increased and decreased with the increase of temperature and it reached maximum at 60 ℃ about 10 mm/y. The polarization curves showed the similar results on corrosion rate of N80 steel after the exposure experiment in CO_2-saturated formation water. Localized corrosion was observed at the temperature of 40 ℃ and 50 ℃. The XRD pattern indicated that the corrosion product was mainly composed by Fe_3C when the temperature under 50℃, then $FeCO_3$ appeared when the temperature was above 50 ℃. At 70 ℃, the corrosion product was comprised of $FeCO_3$ totally. Generally, the temperature of 60 ℃ was the turning point for corrosion type and corrosion product transformation in the test conditions.

1. Introduction

In the process of oil and gas extraction and transportation, CO_2, as an associated gas, can cause serious corrosion to oil casing and gathering pipelines [1-3]. There are many influential factors on the corrosion behaviour of carbon steel in CO_2 corrosion on the formation of corrosion layer, such as temperature, pH, flow rate and etc. [4-6].

It is well recognized that temperature has the great influence in the corrosion process [7-12]. The previous studies have found that the general corrosion rate increases with the temperature increment since the solubility of $FeCO_3$ is high and it is no easy to form protective corrosion film on the surface at lower temperature [7-8]. However, when the temperature was over 60 ℃, the corrosion rate would reduce since the protectiveness of $FeCO_3$ corrosion layer increased with temperature due to the decreased $FeCO_3$ solubility. The formation of corrosion scale was great influence by the temperature. Some studies [7-10] showed that as temperature increased to 60 ℃ to 80 ℃, the corrosion film was more adherent to the substrate and it became more protective to the metal surface. Besides, it is interesting to note that when the temperature was below 40 ℃, the corrosion product was mainly consisted of Fe_3C with some $FeCO_3$. Both Fe_3C and $FeCO_3$ was the corrosion product of CO_2 corrosion [8, 12].

The influence of CO_2 partial pressure has been investigated intensely in recent years [13]. Many researchers have investigated the relationship between CO_2 partial pressure and corrosion rate [14-17].

Generally, higher CO_2 partial pressures result in higher corrosion rates since it can reduce pH and increase the rate of carbonic acid reduction.

The aim of this work was to investigate the corrosion behaviour of N80 steel in the oil formation water with various temperatures. Accordingly, high temperature and high pressure corrosion test was used for weight loss measurement and electrochemical test to study the effect of temperatures in CO_2-saturated formation water.

2. Experimental methods

2.1. Material and solution

In this experiment, N80 steel, with a chemical composition (wt%): C 0.29%, Si 0.26%, Mn 1.11%, P 0.008%, S 0.002%, Mo 0.024%, and Fe balance, was used as experimental material. The microstructure of N80 steel was shown in Figure.1. Specimens were machined with dimensions of 50×13×3 mm^3. Prior to the tests, the working surface of each specimen was abraded within silicon carbide paper of decreasing roughness (up to 800 grit) and rinsed with deionized water followed by alcohol. After drying with cold air, the specimens were weighted using an electronic balance with a precision of 0.1mg and then stored in a desiccator until use. The testing solution contained was prepared from analytical grade reagents and deionized water, simulating the formation water drawn out from an oil field according to Table 1.

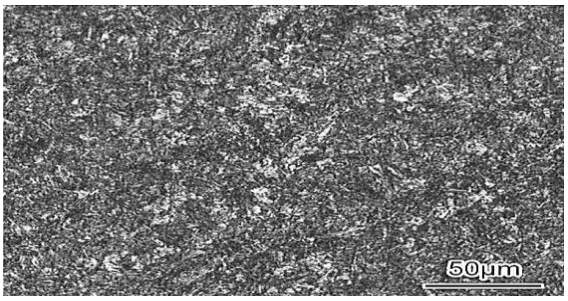

Figure 1. Microstructure of N80 steel

Table 1. Chemical composition of formation water.

Composition	CO_3^{2-}	HCO_3^-	Cl^-	SO_4^{2-}	Ca^{2+}	Mg^{2+}	K^+ and Na^+
Content (mg/L)	28.08	774.8	5405	882.7	1551	13.79	2434.14

2.2. Weight loss test

Corrosion experiments were conducted in a 3 L autoclave to investigate the corrosion rated of N80 steel, and a schematic diagram was presented in Figure 2, which mainly consisted of a gas source supply device, a 3L autoclave, a controller and a waste gas treatment device. As listed in Table 2, the test was designed to determine the effect of temperature on the corrosion behaviour of N80 steel in formation water.

Before the specimens were placed in an autoclave, they were fixed in a specimen holder composed of polytetrafluoroethene (PTFE) to prevent the galvanic effect, and four specimens were placed in the autoclave for each test. Before corrosion test, 2 L formation water, which was deoxygenized by pure N_2 (99.999%) over 12 h, was added to the autoclave. When the autoclave was sealed, purging CO_2 was adopted to remove the air for 2 h. After the autoclave was heated the required temperature, CO_2 gas was injected into the autoclave to 5 MPa.

After the experiments, the specimens were removed from the autoclave, rinsed with deionized water and alcohol and dried with cold air. One of the four specimens was retained for surface characterization of corrosion scales. The rest three specimens were descaled in the solution consisting

of hydrochloric acid, hexamethylene and deionized water at room temperature [18]. The weight loss of the specimen was measured to calculate the general corrosion rate via the following equation [19]:

$$V = \frac{87600 \triangle W}{S \rho t} \tag{1}$$

where V is the corrosion rate, mm/y; ΔW is the weight loss, g; S is the exposed surface area of specimen, cm^2, ρ is the density of specimen, g/cm^3; t is the corrosion time, h; 87600 is the unit conversion constant. The general corrosion rate with error bars was calculated from the three parallel specimens for each test.

Table 2. Test Conditions.

Test	Temperature (℃)	CO_2 Pressure(MPa)	Flow rate(m/s)	Test time (h)
1	30、40、50、60、70	5	1.0	168

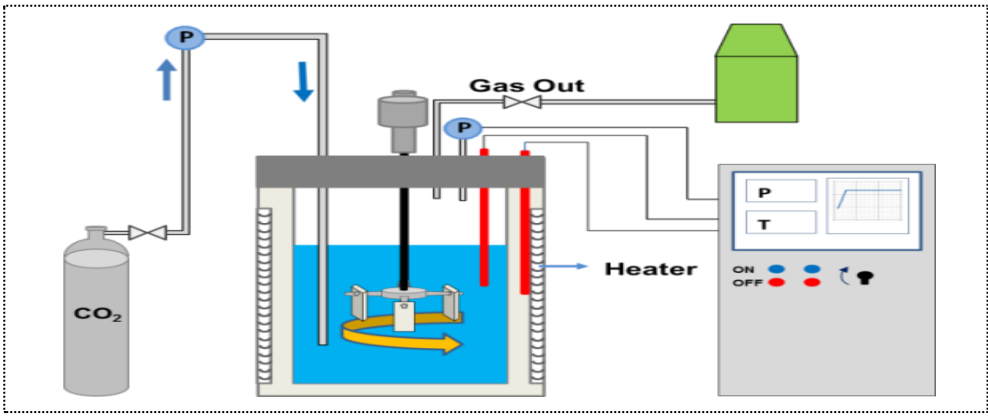

Figure 2. Schematic diagram of the apparatus for the corrosion test.

2.3. Electrochemical test

Electrochemical test was conducted with an electrochemical work station. A three-electrode electrochemical cell was used with N80 steel was working electrode (WE), platinum as counter electrode (CE), and Ag/AgCl electrode (0.1M KCl) as reference electrode (RE). Polarization curve measurements were performed form -0.25 V to 0.25 V vs. OCP with a scan rate 0.5 mVs^{-1}.

2.4. Surface Characterization

After corrosion test, the surface morphologies of corroded specimens were observed by scanning electron microscope (SEM). The composition of corrosion products on the specimen surface was analysed by X-ray diffraction (XRD). The 3D profiles of the samples and sizes of corrosion pits after the removal of corrosion scales were observed and measured using Leica DM 2500M/S6D confocal scanning laser microscope.

3. Results and discussion

3.1. General corrosion rate and macroscopic morphology

Figure 3 shows the weight loss corrosion rate of N80 steel after corrosion in CO_2-saturated water for 168 h. The corrosion of 4 mm/y was recorded at 30 ℃ and it increased until the temperature reached 60 ℃. When the temperature increased to 70 ℃, the general corrosion rate was about 9 mm/y. It can be seen that the general corrosion rate increased initially with the increase of temperature, and then decreased after the temperature of 60 ℃. The general corrosion rate reached maximum about 10 mm/y at 60 ℃.

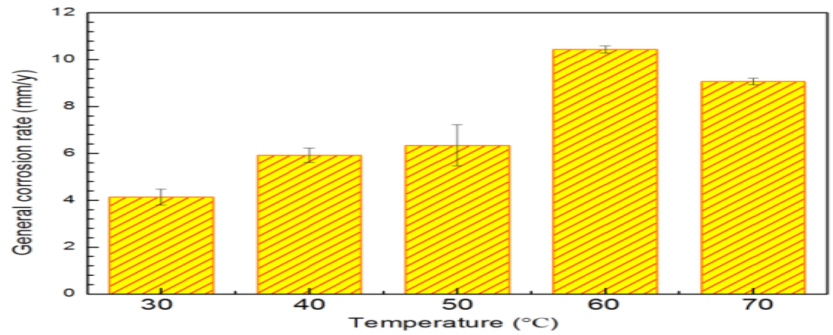

Figure 3. Corrosion rate of N80 steel exposed to CO_2-saturated formation water for 168 h at 5 MPa with various temperatures.

Some studies have shown that the corrosive kinetics of CO_2 has a change near 60 ℃. When the temperature was between 60 ℃ and 110 ℃, a protective layer of corrosion product is formed on the iron surface, which suppresses the corrosion and thus the corrosion rate has a maximum value [7-8].

Figure 4 shows the macroscopic morphologies of corrosion scales on N80 steel. A uniform corrosion film was formed at 30 ℃. With the increase of temperature, some small holes appeared on the corrosion film surface and these holes became more at 50 ℃. When the temperature reached 60 ℃, severe corrosion morphology can be observed in Figure 4d, most of corrosion scale fell off from the matrix and there was small amount of corrosion scale was still remained on the specimen. However, as the temperature increase to 70 ℃, the corrosion scale was almost fell off totally but with a lower general corrosion rate compared to that at 60 ℃.

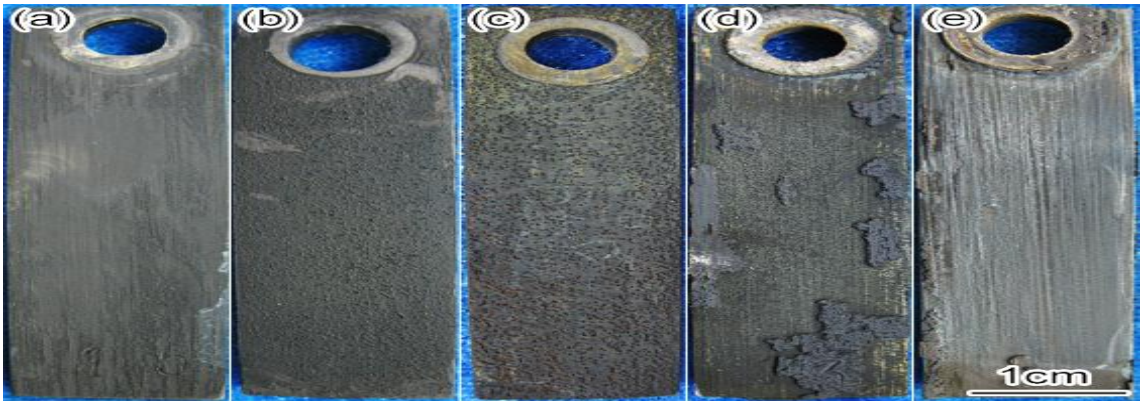

Figure 4. Macroscopic morphologies of corrosion scales on N80 steel exposed to CO_2-saturated formation water for 168 h at 5 MPa with different temperatures:
(a) 30 ℃; (b) 40 ℃; (c) 50 ℃; (d) 60 ℃; (e) 70 ℃.

Compared all the corrosion morphologies with various temperatures, it was found that localized corrosion occurred at 40 ℃ and 50 ℃. The corrosion type was changed from general corrosion to localized corrosion, and then turned to general corrosion finally. The result was in according to other reported studies [14].

3.2. SEM micromorphology and composition analysis

Figure 5 shows the microscopic morphologies of N80 steel exposed to CO_2-saturated formation water for 168 h at 5 MPa with different temperatures. It was observed that some small holes were formed on the corrosion scale at 30 ℃ initially. The holes became larger with the increase of temperature. From the magnification of corrosion morphology, some crystal corrosion product can be found on the surface corrosion layer as shown in Figure 5c to 5e. When the temperature reached 60 ℃, the

corrosion scale became discontinuous and lager crystals were observed compared to that at 50 ℃. This character was still remained at the temperature of 70 ℃.

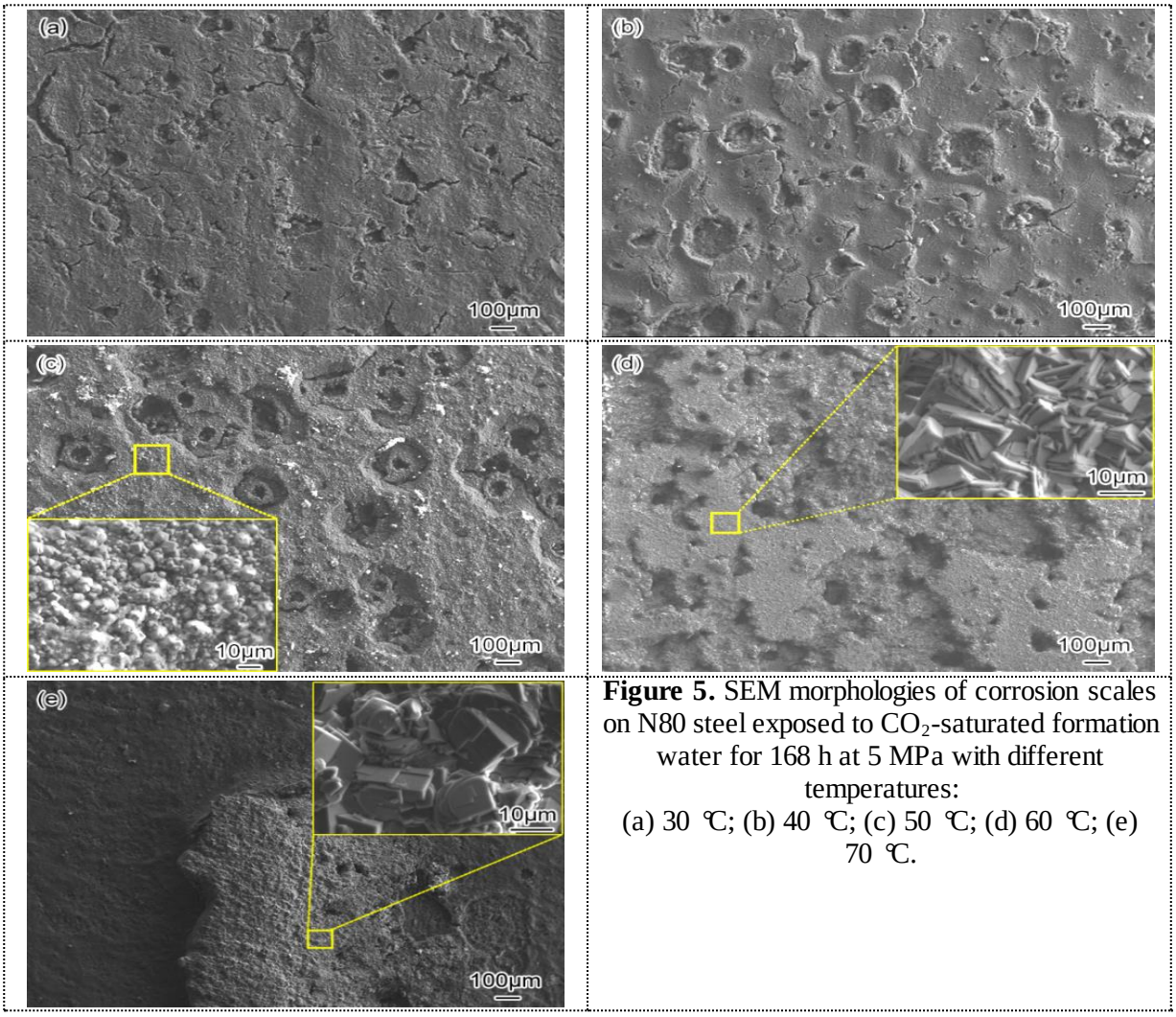

Figure 5. SEM morphologies of corrosion scales on N80 steel exposed to CO_2-saturated formation water for 168 h at 5 MPa with different temperatures: (a) 30 ℃; (b) 40 ℃; (c) 50 ℃; (d) 60 ℃; (e) 70 ℃.

From the microscopic morphologies of N80 steel in different test temperatures, it was obvious that localized corrosion occurred at 40 ℃ and 50 ℃. However, this corrosion type turned to general corrosion when the temperature increases to 70 ℃.

The main corrosion reaction in the CO_2 corrosion process can be summarized as follows:

$$Fe \rightarrow Fe^{2+} + 2e^- \quad (2)$$

$$Fe + HCO_3^- \rightarrow FeCO_3 + 2e^- + H^+ \quad (3)$$

$$Fe + CO_3^{2-} \rightarrow FeCO_3 + 2e^- \quad (4)$$

When the corrosion product film is not formed on the metal surface at the initial stage of corrosion, the anion in the medium can directly react with the metal to form $FeCO_3$ according to the anode reaction (3) and (4). At the same time, the anode reaction (2) causes the dissolution of the Fe^{2+} formed in the matrix into the medium. With the progress of corrosion, when $[Fe^{2+}] \times [CO_3^{2-}]$ in the medium exceeds the solubility product of $FeCO_3$, $FeCO_3$ precipitates on the surface of the sample.

Figure 6 shows the XRD of N80 steel after corrosion in CO_2-saturated formation water for 168 h. It is evident that Fe_3C was primarily detected in the relative low temperature (under 50 ℃). When the

temperature increased to 60 ℃, some $FeCO_3$ crystals were observed in the corrosion products and the corrosion product was comprised of $FeCO_3$ and Fe_3C. However, as the increasing of temperature reached 70 ℃, the corrosion products were mainly composed by $FeCO_3$ and Fe_3C disappeared. In this work, it was interesting to note that $FeCO_3$ formed at 60 ℃. According to some studies [8, 12], both $FeCO_3$ and Fe_3C were two typical corrosion product in CO_2 corrosion. The temperature of Fe_3C formation did not have a certain range while $FeCO_3$ always formed at 50 ℃ to 70 ℃. This was in accordance to the research results.

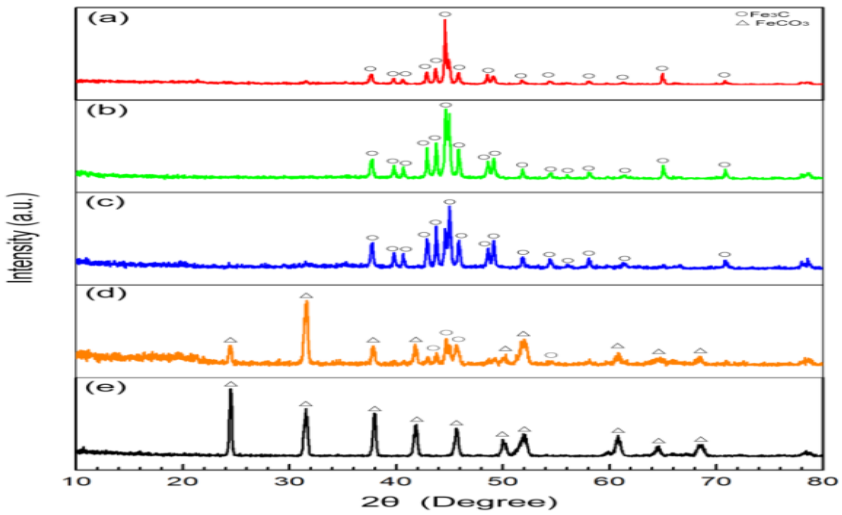

Figure 6. XRD results of corrosion scales on N80 steel exposed to CO_2-saturated formation water for 168 h at 5 MPa with different temperatures: (a) 30 ℃; (b) 40 ℃; (c) 50 ℃; (d) 60 ℃; (e) 70 ℃.

Figure 6 shows the XRD of N80 steel after corrosion in CO_2-saturated formation water for 168 h. It is evident that Fe_3C was primarily detected in the relative low temperature (under 50 ℃). When the temperature increased to 60 ℃, some $FeCO_3$ crystals were observed in the corrosion products and the corrosion product was comprised of $FeCO_3$ and Fe_3C. However, as the increasing of temperature reached 70 ℃, the corrosion products were mainly composed by $FeCO_3$ and Fe_3C disappeared. In this work, it was interesting to note that $FeCO_3$ formed at 60 ℃. According to some studies [8, 12], both $FeCO_3$ and Fe_3C were two typical corrosion product in CO_2 corrosion. The temperature of Fe_3C formation did not have a certain range while $FeCO_3$ always formed at 50 ℃ to 70 ℃. This was in accordance to the research results.

3.3. Localized corrosion analysis and polarization curve measurements

The localized corrosion of N80 steel exposed to CO_2-saturated formation water only occurred at 40 ℃ and 50 ℃. When the temperature was higher or lower than these two conditions, the corrosion type was mainly general corrosion. Figure 7 shows the 3D surface morphologies of the N80 steels at 40 ℃ and 50 ℃, respectively. As shown in Figure 7a, localized corrosion was obvious on the N80 steel, and the depth and diameter of the localized corrosion pits were large at 40 ℃. When the temperature reached 50 ℃, many small localized corrosion pits formed on the steel, while the depth and diameter of the pits were lower than those at 40 ℃.

After the removal of corrosion scale, localized corrosion pits were analysed by the pit depth according to ASTM Standard G46-94 [20]. The localized corrosion rate was calculated by the equation (5):

$$R_L = \frac{8.76h}{t} \tag{5}$$

where R_L is the localized corrosion rate, mm/y; h is the depth of localized corrosion pits, μm. The localized corrosion rate was an average of ten deepest pits obtained from three parallel samples.

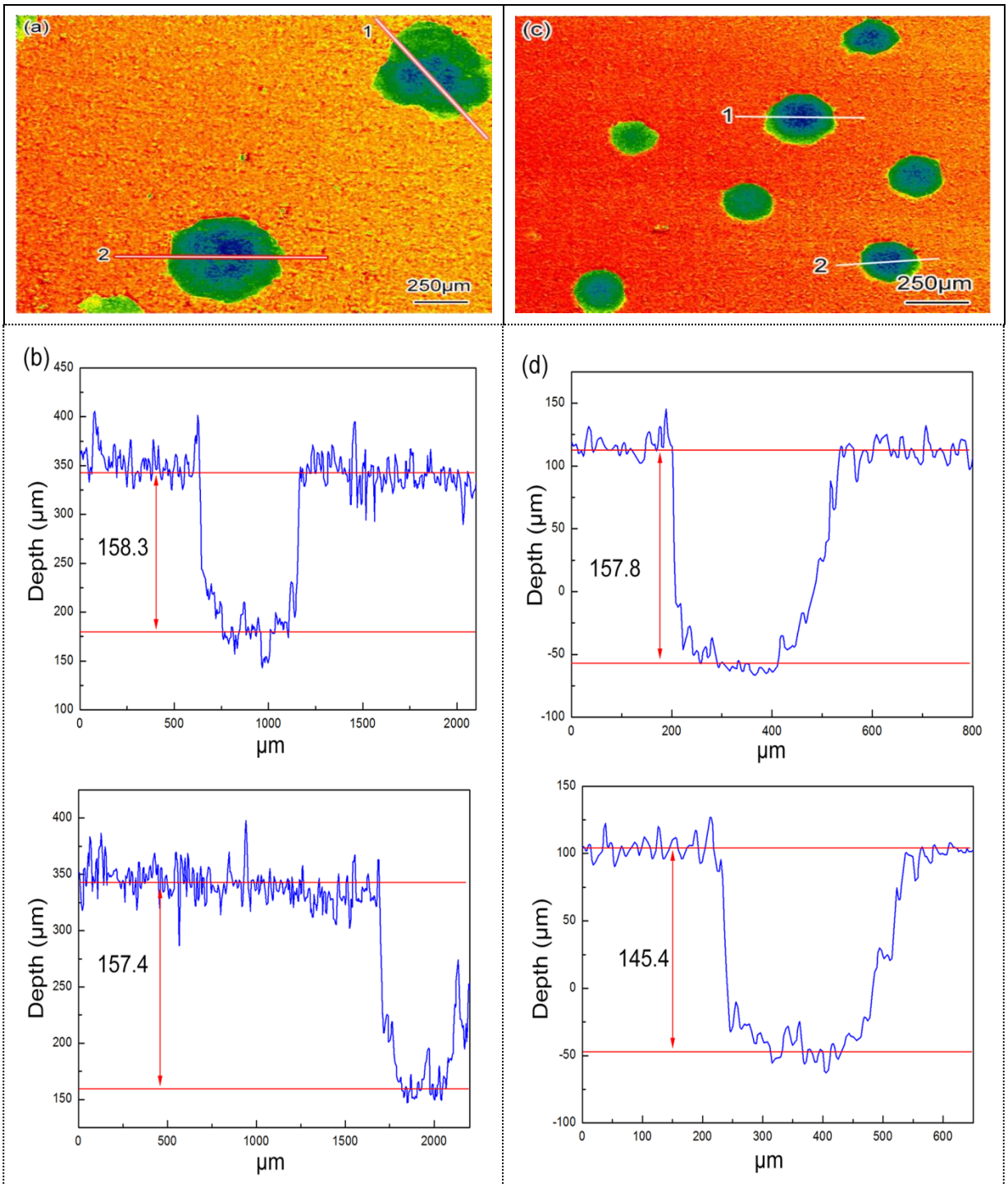

Figure 7. 3D surface morphologies of the N80 steel immersed in CO_2-saturated formation water after 168 h: (a) (b) 40 ℃; (c) (d) 50 ℃.

Figure 8 shows the comparison of corrosion rate on general and localized corrosion at 40 ℃ and 50 ℃. It can be seen that the localized corrosion rate was much higher than that of general corrosion.

When the temperature was 40 ℃, the general corrosion rate was lower than that of 50 ℃, while the localized corrosion rate was a bit higher under 40 ℃. The effect of localized corrosion caused much more damage compared to general corrosion since it would the failure source.

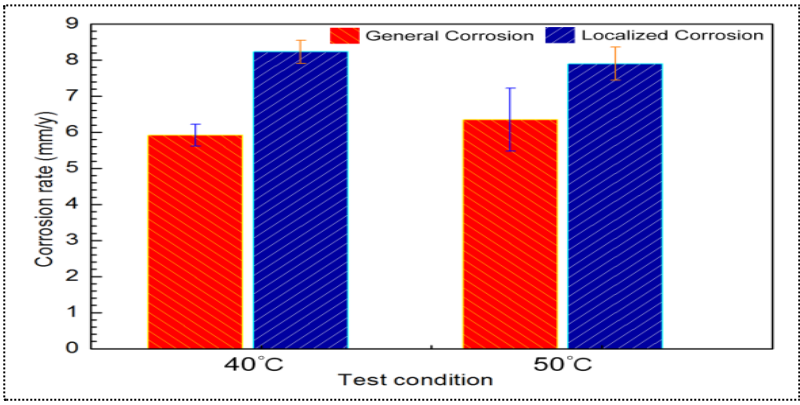

Figure 8. General corrosion rate and localized corrosion rate of the N80 steel immersed in CO_2-saturated formation water after 168h: (a) 40 ℃; (b) 50 ℃.

Figure 9 shows the polarization curves of N80 steel after corrosion in CO_2-saturated formation water. The corresponding values of electrochemical parameters, including corrosion potential and corrosion current density are listed in Table 3. The change of current density under various temperatures was shown in Figure 8b. It is evident that the trend of current density was similar to the general corrosion change varied with temperatures. The current density reached its maximum at 60 ℃ and then decreased to about 5.4 A $\times 10^{-5}$/cm^2.

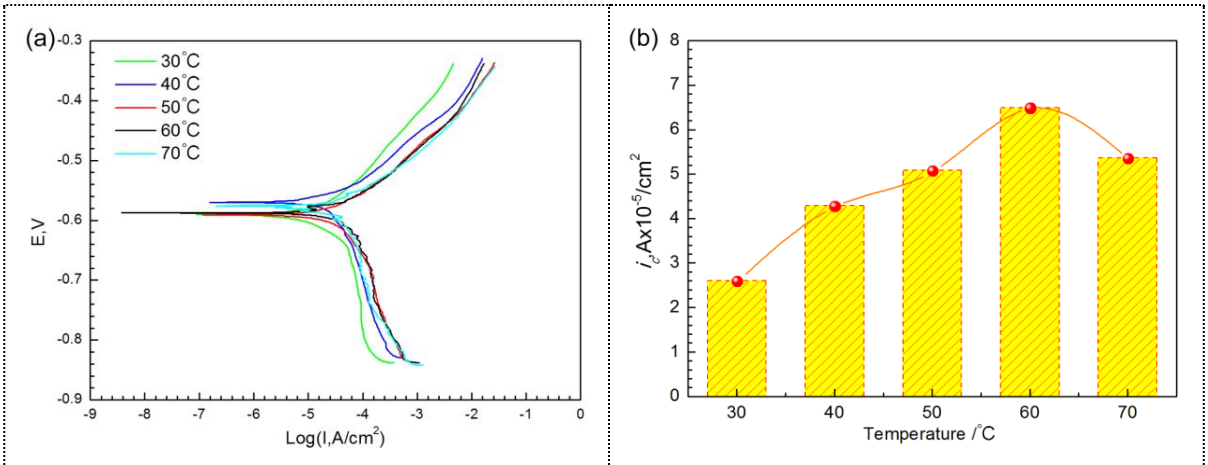

Figure 9. Results of N80 steel for electrochemical measurements in CO_2-saturated formation water:
(a) Polarization curves; (b) Corrosion current density.

Table 3. Fitted electrochemical parameters of the polarization curves of N80 steel after corrosion in CO_2-saturated formation water.

Temperature/ ℃	Corrosion current density i_c/A $\times 10^{-5}$/cm^2	Corrosion potential E_c /mV
30	2.6018	-0.590
40	4.2862	-0.570
50	5.0832	-0.591
60	6.4955	-0.558
70	5.3629	-0.576

4. Conclusions

In this work, the influence of temperature on corrosion behaviour of N80 steel was studied with both high temperature and high pressure corrosion test and electrochemical test. Obtained results showed that the most severe corrosion occurred at 60 ℃ and localized corrosion appeared only at 40 ℃ and 50 ℃. The corrosion products were mainly Fe_3C and $FeCO_3$. The corrosion product was composed by Fe_3C when the temperature under 60 ℃. However, as the increase of temperature reached 60 ℃, $FeCO_3$ was formed, and the corrosion product totally turned to $FeCO_3$ at 70 ℃.

Acknowledgement

This work was supported by the 13th five-year National Science and Technology Major Project of China (2016ZX05016-004), National Natural Science Foundation of China (No. 51701240) and Natural Science Foundation of Shandong Province (No. ZR2017PEM003).

References

[1] Schmitt G 1984 Fundamental aspects of CO_2 corrosion, Advances in CO_2 corrosion, vol. 1, NACE, Houston, TX, pp. 10-19
[2] Kermani M B and Morshed A. 2003 Carbon dioxide corrosion in oil and gas production—A compendium, Corrosion, vol. 59, no.8, pp. 659-683
[3] Crolet J L and Bonis M R 1991 Prediction of the risks of CO_2 corrosion in oil and gas wells, Spe Production Engineering, vol. 6, no. 4, pp. 449-453
[4] Yin Z F, Feng Y R, Zhao W Z, Bai Z Q and Lin G F 2010 Effect of temperature on CO_2 corrosion of carbon steel. Surface & Interface Analysis, vol. 41, no. 6, pp. 517-523
[5] AlSayed and Mohd S A 1989 Effect of flow and pH on CO_2 corrosion and inhibition, Genba Panfuretto vol. 36, no.2, pp. 67-72
[6] Nyborg R 2002 Overview of CO_2 corrosion models for wells and pipelines, CORROSION'02, NACE International, Houston, TX, paper no. 233
[7] Dugstad A 1998 Mechanism of protective film formation during CO_2 corrosion of carbon steel, CORROSION'98, NACE International, Houston, TX, paper no. 31
[8] Muñoz A, Genesca J, Duran R and Mendoza J 2005 Mechanism of $FeCO_3$ formation on API X70 pipeline steel in brine solutions containing CO_2, CORROSION'05, NACE International, Houston, TX, paper no. 297
[9] Bosch C, Jansen J P and Poepperling R K 2003 Influence of chromium contents of 0.5% to 1.0% on the corrosion behaviour of low alloy steel for large-diameter pipes in CO_2 containing aqueous media, CORROSION'03, NACE International, Houston, TX, paper no. 118
[10] Dugstad A, Lunde L and Videm K 1994 Parametric study of CO_2 corrosion of carbon steel, CORROSION'94, NACE International, Houston, TX, paper no.14
[11] Sui P F, Sun J B, Hua Y, Liu H F, Zhou M N, Zhang Y C, Liu J H and Wang Y 2018 Effect of temperature and pressure on corrosion behaviour of X65 carbon steel in water-saturated CO_2 transport environments mixed with H_2S, Int J Greenh Gas Con, vol. 73, pp. 60-69
[12] Jasinski R 1987 Corrosion of N80-type steel by carbon dioxide/water mixtures, Corrosion, vol. 43, pp. 214-218
[13] Dugstad A, Lunde L and Videm K 1994 Parametric study of CO_2 corrosion of carbon steel, CORROSION'94, NACE International, Houston, TX, paper no.14
[14] Sun Y and Nesic S 2004 A parametric study and modelling on localized CO_2 corrosion in horizontal wet gas flow, Corrosion'04, NACE International, Houston, TX, paper no. 380
[15] Kinsella B, Tan Y J and Bailey S 1998 Electrochemical impedance spectroscopy and surface characterization techniques to study carbon dioxide corrosion products, Corrosion, Vol. 54, pp. 835-842
[16] Fu S L and Bluth M J 1994 Study of sweet corrosion under flowing brine and/or hydrocarbon conditions, CORROSION '94, NACE International, Houston, TX, paper no. 31

[17] Hesjevik S M and Olsen S 2003 Corrosion at high CO_2 pressure, CORROSION'03, NACE International, Houston, TX, paper no. 03345
[18] ASTM Standard G1-03 2011 Standard Practice for Preparing, Cleaning, and Evaluating Corrosion Test Specimens. ASTM International, West Conshohocken, PA
[19] ASTM Standard G31-72 2004 Standard Practice for Laboratory Immersion Corrosion Testing of Metals. ASTM International, West Conshohocken, PA
[20] ASTM Standard G46-94 2003 Standard guide for examination and evaluation of pitting corrosion. ASTM International, West Conshohocken, PA